The Uranium Recovery from Aqueous Solutions Using Amidoxime Modified Cellulose Derivatives. II. Uranium Uptake Behavior of Amidoximated Ethyl Cellulose

Seyhan Şener Başarır, Nursel Pekel Bayramgil ✉ iD *

Hacettepe University, Faculty of Science, Chemistry Department, 06800, Beytepe, Ankara, Turkey

Abstract: Amidoxime modified ethyl cellulose (EC-*g*-AO) was utilized to recover uranyl ions from aqueous solutions through a process of complexation. Adsorption trials were carried out at varying UO_2^{2+} concentrations ranging from 100 to 1000 mg/L and at temperatures ranging from 25 to 50°C. Thermodynamics and kinetics of the adsorption of uranyl ions (UO_2^{2+}) by EC-*g*-AO were examined. The findings suggested an adsorption capacity of 240 mg UO_2^{2+}/g dry copolymer. Thermodynamic parameters applicable to the interaction of UO_2^{2+} with EC-*g*-AO were calculated from thermodynamic relations. Calculations indicated that adsorption took place through powerful electrostatic interactions with an enthalpy of -23.6 kJ/mol. UO_2^{2+} desorption was investigated by desorption agents like EDTA, HCl, $NaHCO_3$, and NaOH. The desorption yield found for $NaHCO_3$ was 52%.

Keywords: Ethyl cellulose, uranium, $NaHCO_3$, adsorption enthalpy, EDX.

INTRODUCTION

Seawater contains abundant dissolved alkali and rare earth alkali metal ions, alongside a lesser amount of some valuable metals like lithium and uranium (1). The relevant literature (2-5) features numerous studies related to the removal of heavy metal ions from seawater and wastewater, especially for the selective recovery and the enrichment of uranyl ions.

Being toxic and radioactive, uranium poses a risk for both surface and underground waters. On the other hand, uranium is utilized as a raw material for nuclear power plants and has had a tremendous commercial significance. Nevertheless, as the uranium reserves are anticipated to be depleted in the near future, studies have focused on the recovery of uranium from natural water sources ($0.1–10$ mg U/m^3), especially from sea water ($2.8–3.3$ mg U/m^3). Various organic adsorbents containing different functional groups or organic chelates that are more or less selective towards uranium were synthesized and used to recover uranium from seawater or mining wastewaters (6-9). The desired properties of these chelates are high capacity, high selectivity, fast kinetics, high mechanical strength, and a fast equilibrium established with metal ion solution. Notably, amidoxime containing synthetic and natural polymers are the most promising systems for the uranium recovery (10). From past to present, a number of studies were published on the adsorption of uranyl ions by polymers and copolymers containing amidoxime functional groups (11-14).

Neti *et al*. (15) reported their effort to induce hydrophilicity in the support polymer through the grafting of a hydrophilic monomer onto PE prior to ATRP polymerization of acrylonitrile and 2-hydroxyethyl acrylate. The prepared adsorbents demonstrated promise (159.9 g U/kg of adsorbent) in laboratory screening tests using a high uranium concentration brine and 1.24 g U/kg of adsorbent in the filtered natural seawater in 21 days. Abney *et al.* (16) published a review of inorganic and organic materials used in the recovery of uranium from seawater and their detailed synthesis methods. He mentioned that amidoxime-functionalized polymers are the most technologically ripe adsorbent for the uranium recovery and have indicated impressive performance following protracted contact with seawater in screening studies, as well as in long-term dehiscence at the pilot scale in the open ocean. In another study (17), uranyl ion uptake from sulfuric acid solutions has been evaluated as a function of pH and sulfate concentration, with comparison to a commercially available weak base anion exchange resin. Maximum uranyl loading capacity was found as 269.50 mg/g for weak base anion exchange resin.

It is well known that currently available adsorbents require security measures and a sophisticated installation process, and they are more expensive than water treatment. Due to such constraints and environmental issues, there is a growing interest in the use of biomass for the removal of dissolved metals. For this purpose, numerous low-cost biomasses have been developed and commercially utilized to control pollution (18-21). Examples to low-cost

adsorbents include activated carbon, clay, agricultural waste, tea leaves, cellulose, fly ash, wool fiber, animal bones, immobilized fungal biomass, peanut shell pellets, and pineapple shells. Among them, cellulose has attractive properties; it is biodegradable, biocompatible, highly abundant, cheap, and it has been obtained from renewable resources. Cellulose interacts with soil microorganisms, transforms into eco-friendly end products, CO_2 and H_2O, and does not cause secondary pollution; thus, it is superior to synthetic polymers (22,23).

In our previous study, we synthesized graft copolymers consisting of ethyl cellulose (EC) and acrylonitrile (AN) through high-energy radiation. Details concerning the characterization and yield of grafting and amidoxime conversion were provided in this previous study (24). This study aimed to investigate how UO_2^{2+}- and amidoxime-modified ethyl cellulose interacted within a certain temperature range, and it also revealed some conclusions about the physicochemical quantities that are effective in the specific adsorption process. These interactions were investigated as a function of temperature based on adsorption isotherms. The enthalpy, entropy, activation energy, and Gibbs free energy parameters of UO_2^{2+} adsorption were calculated from basic thermodynamic equations. Different releasing agents including HCl, EDTA, $NaHCO_3$ and NaOH were tested for desorption studies. Morphological, structural, and thermal changes were monitored through SEM-EDX, FTIR/ATR, and TGA, respectively.

MATERIALS AND METHODS

Materials
Ethyl cellulose (Sigma-Aldrich Chemie GmbH, Germany) and acrylonitrile (Aldrich, Germany) were used as received. Hydroxylamine hydrochloride and sodium hydroxide were supplied from Riedel de Haën and Merck, respectively.

Uranyl nitrate, $UO_2(NO_3)_2.6H_2O$ (purity$\geq$98%) (BDH Chemicals Ltd., Poole, U.K.) was utilized as the source of uranyl ions. Sodium salicylate, HOC_6H_4COONa (analytical grade), which forms a complex with UO_2^{2+} for UV spectrophotometric measurements, was obtained from Fischer Scientific, U.K.

Synthesis of ethyl cellulose and acrylonitrile graft copolymers
Ethyl cellulose (EC) and acrylonitrile (AN) graft copolymers (EC-*g*-AN) were synthesized by irradiating various initial feed compositions of EC and AN through ^{60}Co-γ irradiator at room temperature. The conversion of initial mixtures into crosslinked, insoluble structures was determined gravimetrically after the copolymers kept in dimethyl formamide for a period of one week in order to extract the unreacted monomers and uncrosslinked soluble fractions. With 100% success, nitrile groups were converted into amidoxime groups in a neutralized $NH_2OH.HCl$ solution at 50 °C. The details concerning the characterization, radiation synthesis, and amidoximation of EC-*g*-AN copolymers were reported in our previous study (24).

Adsorption of UO$_2$$^{2+}$ onto amidoxime (AO) modified ethyl cellulose (EC-*g*-AO)

Approximately 0.25 g of EC-*g*-AO copolymers in cylindrical form (~0.5 cm in length) were immersed into 25 mL UO$_2$$^{2+}$ solutions at concentrations varying from 100 to 1000 mg/L (pH 4.1). In a thermostatically controlled water bath, the solutions were shaken in closed flasks at 25 °C ± 0.5 °C. 0.5 mL aliquot was taken and sodium salicylate was added to form a complex during the shaking process. Then, the absorbance of this solution was recorded at 429 nm using a Jasco V-530 model UV-vis spectrophotometer and concentration changes were read from a previously obtained calibration curve. The adsorption equilibrium was achieved in 7-10 days. We repeated the adsorption trials following the same experimental route at other temperatures (30°C, 40°C, and 50°C). The adsorbed amount of UO$_2$$^{2+}$ was calculated with the equation (1):

$$q_e = \frac{V}{m} x (C_0 - C)$$ (Eq. 1)

Where q_e is the amount of adsorbed UO$_2$$^{2+}$ (mg UO$_2$$^{2+}$ / g dry EC-*g*-AO), V is the volume of the UO$_2$$^{2+}$ solution (L), m is the dry weight of EC-*g*-AO (g), and C$_o$ and C are the initial and equilibrium concentrations of UO$_2$$^{2+}$ (mg/L), respectively.

The kinetics and thermodynamic quantities as activation energy (E$_a$), adsorption enthalpy (ΔH°$_{ads}$), Gibbs free energy of adsorption (ΔG°$_{ads}$), and entropy of adsorption (ΔS°$_{ads}$) were calculated based on the below-given classical equations, respectively:

$$k = A.e^{-\frac{E_a}{RT}} \qquad \text{Arrhenius equation} \quad \text{(Eq. 2)}$$

$$\Delta G^0_{ads} = -RT ln K_L \qquad \text{Gibbs free energy (Eq. 3)}$$

$$ln K_L = -\Delta H^0/RT + \Delta S^0/R \qquad \text{Gibbs-Helmholtz equation (Eq. 4)}$$

Desorption of UO$_2$$^{2+}$ from EC-*g*-AO copolymers using different agents

Solutions each of which having the concentration of 0.1 M EDTA, NaOH, HCl, and NaHCO$_3$ functioned as desorption agents in order to release adsorbed UO$_2$$^{2+}$ from EC-*g*-AO copolymers. EDTA was provided by BDH; and the other three were obtained from Merck, Darmstadt, Germany. Also, desorption was carried out at pH 4.1. UO$_2$$^{2+}$ adsorbed EC-*g*-AO copolymers were placed, separately and in predetermined amounts, into the aforementioned solutions, and the concentration of released UO$_2$$^{2+}$ was measured in regular intervals with the UV-Vis spectrophotometer at 429 nm. Desorption (%) values were calculated in the following manner:

$$Desorption\ (\%) = \frac{amount\ of\ released\ UO_2^{2+}}{total\ amount\ of\ adsorbed\ UO_2^{2+}} x 100$$ (Eq. 5)

Thermal, spectroscopic, and morphological analyses of UO$_2$$^{2+}$ adsorbed EC-*g*-AO

We directly recorded the FTIR/ATR spectra of EC-g-AO copolymers with and without UO$_2$$^{2+}$ in a 4000-400 cm^{-1} range and took a total of 10 scans at 4 cm^{-1} resolution. A Nicolet IS10 Model FTIR/ATR spectrometer was used for this operation. We examined UO$_2$$^{2+}$ adsorbed EC-*g*-AO's

thermal behavior with a DTG-60H Shimadzu (Simultaneous DTA-TG Apparatus) thermogravimetric analyzer in N_2 atmosphere; the temperature range was 0-700 °C and the heating rate was 10°C/min. The flow rate of N_2 gas was 60 mL/min. SEM images of UO_2^{2+} adsorbed EC-g-AO copolymers were obtained with Quanta 200 FEG SEM-FEI Model Scanning Electron Microscope, which enabled an observation of morphological changes at an accelerating voltage ranging from 10.00 kV to 15.00 kV. We ensured the conductivity of polymer samples by gold-coating. A simultaneous analysis of SEM and EDX (Energy Dispersive X-Ray Spectroscopy) with Bruker Electron Microscope enabled the elemental analysis of UO_2^{2+} adsorbed EC-g-AO copolymers.

RESULTS AND DISCUSSION

Detailed information regarding the amidoxime conversion, radiation synthesis, and characterization of EC-g-AO copolymers were presented as another study (24). EC-g-AO copolymers were subjected to adsorption experiments in order to determine their UO_2^{2+} uptake capacity, which is explained in the experimental section. For the adsorption kinetics studies, copolymer samples were removed from UO_2^{2+} solutions at regular intervals and complexed with sodium salicylate. Then, using a UV-Vis spectrophotometer, the absorbance of orange-colored complexes was recorded at 429 nm.

The ion-exchange mechanism for UO_2^{2+}, which binds to the polymer, is complicated by the hydrolyzation of UO_2^{2+} in an aqueous solution within the pH range of the examined adsorption system, and different types of hydrolyzed UO_2^{2+} species are formed. UO_2^{2+} species are dominant in pH 1-4 range. At pH 4, the presence of $UO_2(OH)^+$ within the solution remains around 2.2%; the maximum value of which rises to 18.6% at pH 6. The presence of $UO_2(OH)_2$ within the solution – maintained at pH 4 – is approximately 1.5%. UO_2^{2+} and H_3O^+ compete in the solution within the range of pH 1-4. As the aqueous solution's pH value rises from 1 to 4, UO_2^{2+} adsorption increases, whereas the adsorption of H_3O^+ decreases. Above pH 4, the hydrolysis of UO_2^{2+} triggers the formation of $UO_2(OH)_2$, $UO_2(OH)^+$, and $UO_2(OH)_3^+$ species (25). Based on these evaluations, we kept the pH value at constant 4.1 (own value of UO_2^{2+} solution). Below this value, we observed some distortions in the geometry of amidoximated copolymer, and even better UO_2^{2+} adsorption values were obtained. Some hydroxyl species formed above this limit pH value. During the whole adsorption experiments, this pH value was not affected with the presence of neutral ethyl cellulose copolymers although very few fluctuations occurred within pH 4-4.5.

Figure 1 shows the decrease in UO_2^{2+} concentrations in time for constant composition of EC-g-AO (the initial composition of 0.6 g EC in 6 mL acrylonitrile (AN) were used in our previous paper) copolymers for different initial UO_2^{2+} concentrations at 25°C (at pH 4.1). Using first order kinetic model, the initial rates (- d[UO_2^{2+}]/dt = r_i), calculated based on the initial slope of those

curves shown in Figure 1, are presented in Table 1, for each temperature, as a function of the initial UO_2^{2+} concentration. Table 1 demonstrates that the **r_i** of interaction between UO_2^{2+} and amidoxime groups increases with increasing concentration of UO_2^{2+} at a given temperature. In addition, contrary to what we know about the physical and chemical adsorption, the UO_2^{2+} adsorption increases with rising temperatures. This is because the structure of ethyl cellulose contains plenty of OH groups that link the glucose units layered. Rising temperature may cause some of these bonds to be broken and the rigidity of ethyl cellulose is decomposed to a certain extent. The adsorption rate of UO_2^{2+} on copolymers increases, enabling access to amidoxime groups.
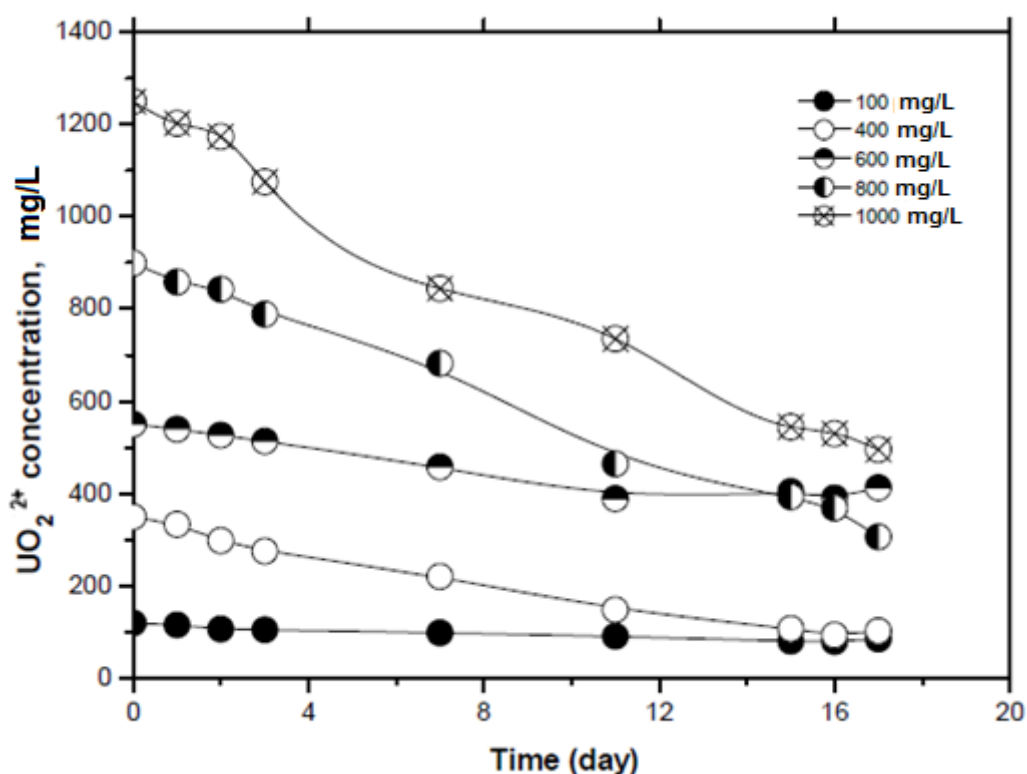
Figure 1. Kinetics of UO_2^{2+} adsorption at different UO_2^{2+} concentrations (0.6 g EC dissolved in 6 mL of AN; 25°C; pH 4.1)

**Table 1.** Initial rates and rate constants calculated from kinetic data.

Temperature	Initial conc. of UO_2^{2+} (mg/L)	initial conc. of UO_2^{2+} ($\times 10^4$ mol/L)	Initial rate, r_i ($\times 10^6$ mol/L.h)	rate constant, k ($\times 10^4$ 1/h)
25 °C	400	14.80	2.34	
	600	22.22	3.76	5.1
	800	29.62	4.43	
	1000	37.03	4.96	
40 °C	400	14.80	4.32	
	600	22.22	4.96	6.6
	800	29.62	7.13	
	1000	37.03	8.63	
50 °C	400	14.80	4.87	
	600	22.22	6.39	7.3
	800	29.62	8.24	
	1000	37.03	9.79	

Calculated **E_a** value from Arrhenius equation **= 43.04 kJ/mol**

Certain amounts of EC-*g*-AO copolymers were added to varying concentrations of UO_2^{2+} solutions at known volume and shaken for a predetermined period (around 10 days). This process continued until the adsorption equilibrium was reached. The equilibrium amounts of adsorbed UO_2^{2+} were calculated based on Equation 1. The adsorption capacity values of UO_2^{2+} mg/g dry copolymer were plotted versus equilibrium concentrations (**C_e**) of UO_2^{2+} to obtain adsorption isotherms for each temperature studied. From Figure 2, the adsorption isotherms demonstrate a high-affinity type (26) behavior due to the strong interaction between UO_2^{2+} and amidoxime groups for all temperatures. The shape of the isotherms shows that the same amount of UO_2^{2+} adsorption takes place in all active regions of EC-*g*-AO copolymers. In other words, adsorption takes place when the specifically adsorbed amount of ionic species on solid polymer exceeds that of ionic species found in the solution (27). To put it another way, copolymer gives a specific and strong significance to uranium; adsorption takes place very fast initially, then slows down as the sites available for adsorption decrease. This is the usual case for Langmuir isotherm. The linearized Langmuir equation (28) enables one to determine a significant parameter representing a measurement of the chelating resin-binding capacity for a given species [**K_L**, the equilibrium-binding constant (**k_{ads}/k_{des}**)]. The linearized form of Langmuir equation is presented in Equation (6):

$$\frac{C_e}{q_e} = \frac{1}{K_L q_s} + \frac{C_e}{q_s} \qquad\qquad \text{(Eq. 6)}$$
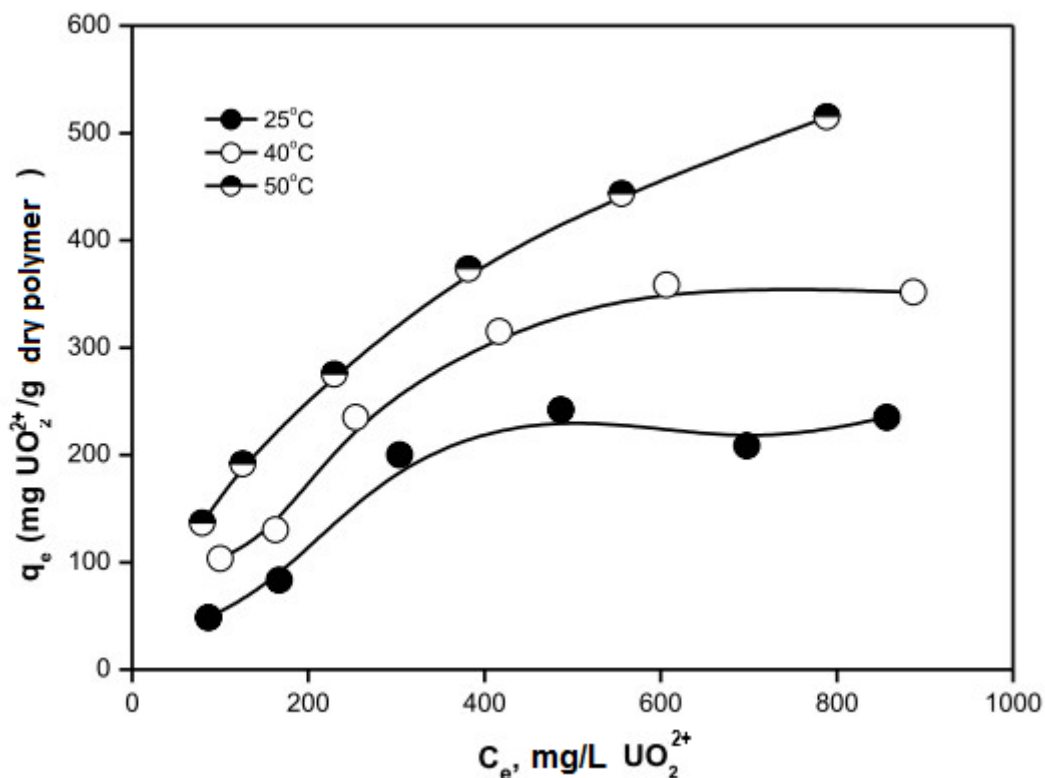
Figure 2. Adsorption isotherms obtained at different temperatures.

The K_L values obtained for Ec-*g*-AO copolymers are listed in Table 2 with q_e values. Despite the fact that UO_2^{2+} adsorption rose at higher temperatures, K_L values indicated the genuine results: The desorption rate remained high at high temperatures for K_L values from 25 to 50°C. Equations 2-4 and 6 are interpreted together in order to calculate the thermodynamic parameters of UO_2^{2+} adsorption. Activation energy, entropy, enthalpy, and Gibbs free energy values applicable to the UO_2^{2+} adsorption onto EC-*g*-AO copolymers were demonstrated in Tables 1 and 2. Calculated from Equation 2, E_a (43.04 kJ/mol) indicates that the adsorption of UO_2^{2+} by EC-*g*-AO copolymers has taken place through an internal diffusion-controlled process for chemical adsorption (30-120 kJ/mol) (29). Moreover, the other thermodynamic parameters calculated using Eq. 2-4 confirmed the powerful interaction between amidoxime groups and UO_2^{2+}, and such interactions have been demonstrated for exothermic favorability. In our study, the most important parameter that determines the tendency of a spontaneous event, Gibbs free energy, ΔG_{ads}, has a negative value. In addition, ΔH_{ads} value has been found as -23.61 kJ/mol. This is very close to the threshold of the enthalpy of chemical adsorption and that of the physical adsorption. Adsorption happens physically at $\Delta H_{ads} << -40$ kJ/mol and chemically at $\Delta H_{ads} > -40$ kJ/mol. Although the interaction between UO_2^{2+} and amidoxime groups takes place with the aim of physical forces, binding between the two is quite strong. Desorption studies support our findings in this context.

Table 2. Thermodynamic parameters of UO_2^{2+} adsorption onto EC-*g*-AO copolymers

| Temperature (°C)	q_e (mg/g)	K_L (Langmuir eqn.)	$-\Delta G_{ads}$ (kJ/mol, Gibbs eqn.)	ΔS_{ads} (J/K mol, Gibbs-Helmholtz eqn.)
25	24	523	15.51	27.18
40	35	292	14.07	30.48
50	51	255	13.73	30.60

ΔH_{ads} **= -23.61 kJ/mol**   (Gibbs-Helmholtz eqn.)

The relevant literature (12-14,30,31) contains many studies conducted on both amidoximated resin and unmodified biomass, separately, for the uranium recovery. But none of them included the uranium recovery by amidoximated biomass. In some studies, the modification was achieved by some acid groups (13), and in others, those heavy metal ions other than uranium (10) were used, or they presented only the synthesis and characterization. Therefore, direct study was not present for the uranium recovery by amidoximated cellulose. Only in one study performed by Badawy et al. (7) the authors showed that acrylonitrile/methacrylic acid grafted cotton cloths can be used to recover uranium from aqueous systems with an adsorption capacity of 662 μg/g. This value is a rather small value from the value obtained in our study (240 mg/g).

To be able to explain the mechanism by which UO_2^{2+} binds to amidoxime groups, FTIR/ATR spectra of UO_2^{2+} adsorbed EC-*g*-AO copolymers were obtained, which are shown in Figure 3. Because of interactions with UO_2^{2+}, there are some shifts on some characteristic bands. The band for C=N belonging to amidoxime group at 1660 cm^{-1} shifts by approximately 15 cm^{-1}, and also there is an 8 cm^{-1} shift for N-O stretching vibrations at 912 cm^{-1}. The band intensity at 1550 cm^{-1}, attributed to C-N group of amidoxime, increased, and it got clearer after UO_2^{2+} adsorption. Other band shifts occur at 3200 cm^{-1} for the interaction of both =N-OH and –NH$_2$ (of amidoxime) groups with UO_2^{2+}. This suggests that UO_2^{2+} on EC-*g*-AO copolymers is absorbed through both –C-NH$_2$ and –C=N-O-H segments of amidoxime, and the mechanism is proposed as in scheme 1:
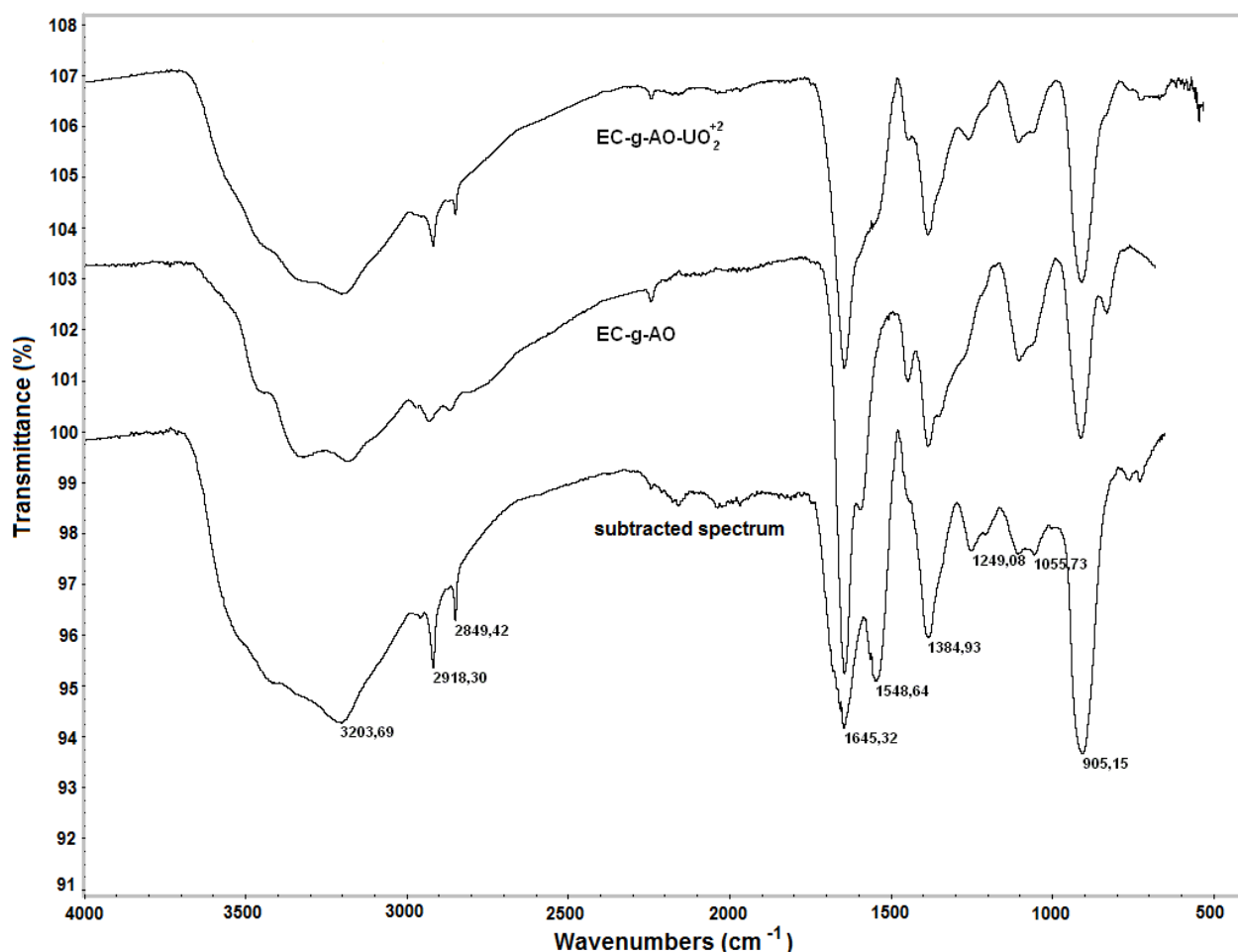
Figure 3. FTIR/ATR spectra of EC-*g*-AO copolymers before and after UO_2^{2+} adsorption
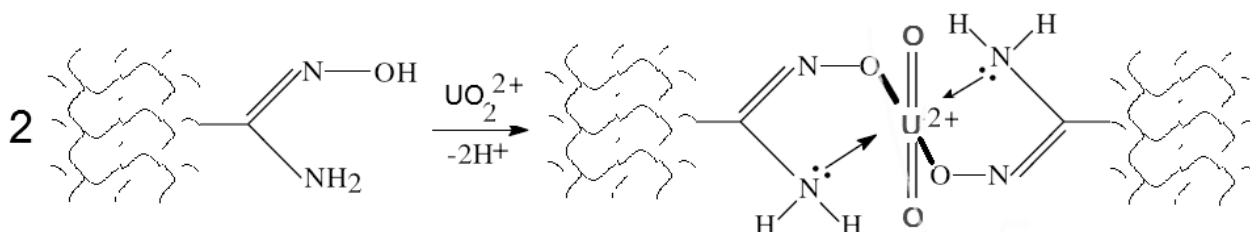

Scheme 1. Coordination of amidoxime group to uranyl cation.

Another similar mechanism was observed as part of the study of adsorption of metal ions by amidoxime-modified synthetic resins (32). Given the bidentate character of amidoxime groups, two amidoxime groups hold an UO_2^{2+} as a clamp and ensure 6-coordination.

Thermal analyses were performed to account for the thermal behavior of EC-*g*-AO after UO_2^{2+} adsorption. Evaluations of EC-*g*-AN copolymers in terms of TGA and derivative TGA before and after amidoxime conversion were reported in another study of ours (24). Figure 4 presents TGA,

der.TGA, and DTA thermograms for UO_2^{2+} adsorbed EC-*g*-AO copolymer. As can be seen in the figure, there are different steps of decomposition upon the adsorption of UO_2^{2+}. Due to the interaction between the amidoxime group and UO_2^{2+}, the level of decomposition observed at 275 °C corresponded to the amidoxime groups and the decomposition at 433 °C corresponded to cellulosic structures. The addition of C≡N (nitrile) groups affected it, leading a slight increase in the cellulose's stability. The decompositions observed at 462°C, 508°C and 621°C probably show the decompositions of some groups which interacted with UO_2^{2+}. The last three decompositions were not observed in the TGA thermogram of EC-*g*-AO copolymer itself (24). The EC-*g*-AO copolymer lost approximately 90% of its weight throughout the heating process that continued up to 700°C. Since the UO_2^{2+} did not diffuse thoroughly into the crystalline cellulose by defeating strong H-bonds, it would not access to all adsorption sites, and the adsorption amounts of UO_2^{2+} is lesser compared to the other studies in the literature (33-35). As a result, such a high weight loss arose from carbonization of cellulosic units. When the residue of TGA was analyzed, it was shown that the structure belongs to U_3O_8 (36).
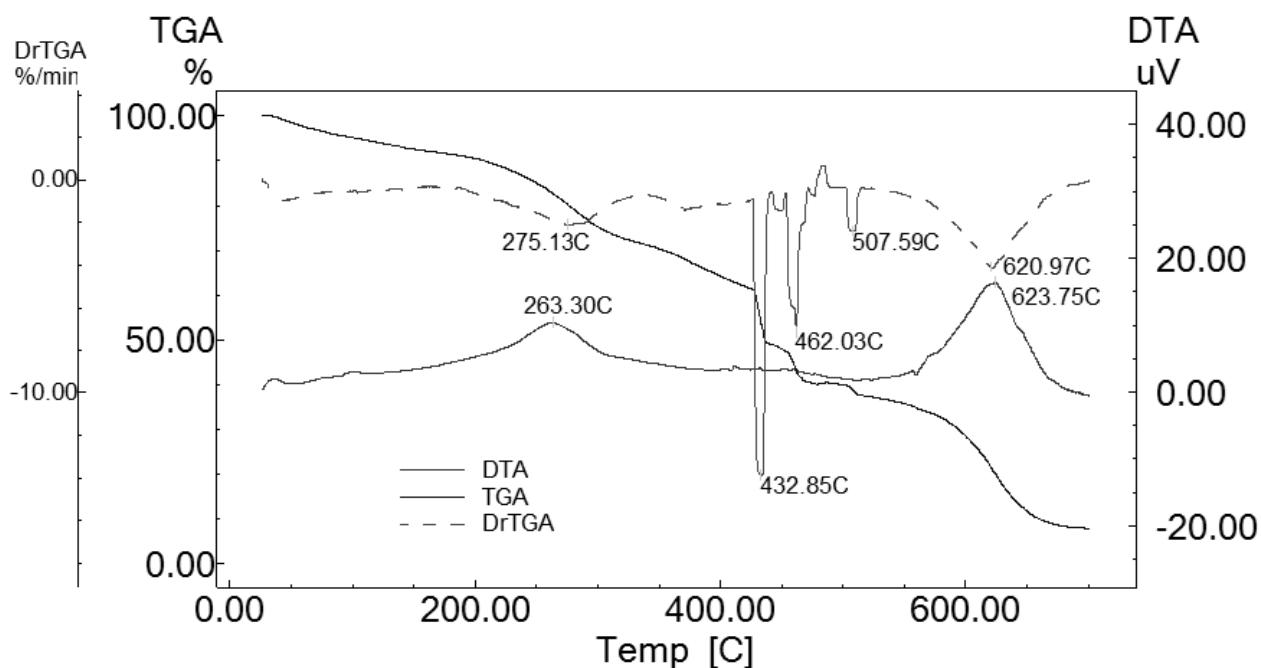

Figure 4. TGA thermogram of EC-*g*-AO copolymers after UO_2^{2+} adsorption.

SEM and SEM-EDX images were obtained to analyze the surface morphology of EC-*g*-AO copolymers following UO_2^{2+} adsorption. The Scanning Electron Microscopy (SEM) enables an observation of the materials' topographic features as 3-D images, whereas the Energy Dispersive X-Ray Spectroscopy (EDX) allows performance of an elemental analysis on the materials' microscopic sections. The SEM images of EC-*g*-AO copolymers, before and after UO_2^{2+} adsorption, are provided in Figure 5. As shown in the figure (b,c), there are highly visible orthorhombic bipyramidal crystal structures of UO_2^{2+}. In the colored figure, bright regions observed around crystals indicates that radioactive heavy metal ion is attached to the structure.

SEM images were taken to analyze if the UO_2^{2+} is connected to EC-*g*-AN copolymer before amidoxime conversion (Figure 5(a)). As can be clearly seen, the absence of UO_2^{2+} crystals on the topological image of EC-*g*-AN copolymer confirmed that the unamidoximated copolymer did not adsorb UO_2^{2+}. This draws attention to similar crystal occurrences on the surface, reported by Allen and Tempest (37). The orthorhombic bipyramidal crystal structure of UO_2^{2+}, which is seen on the copolymer surface, is presented in Scheme 2:
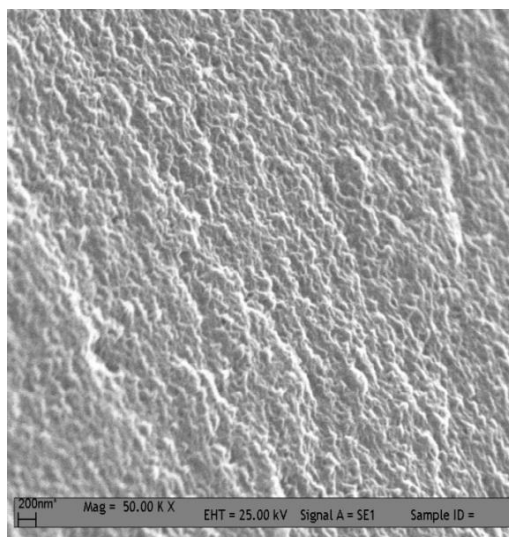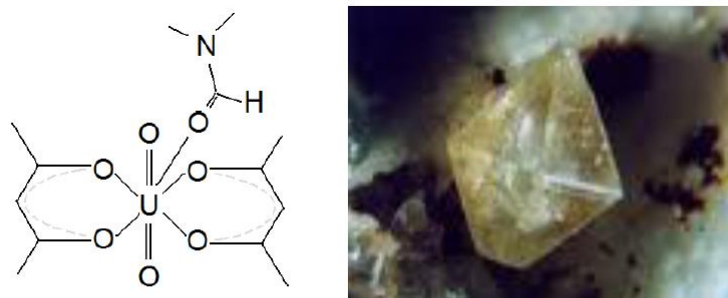

(a)
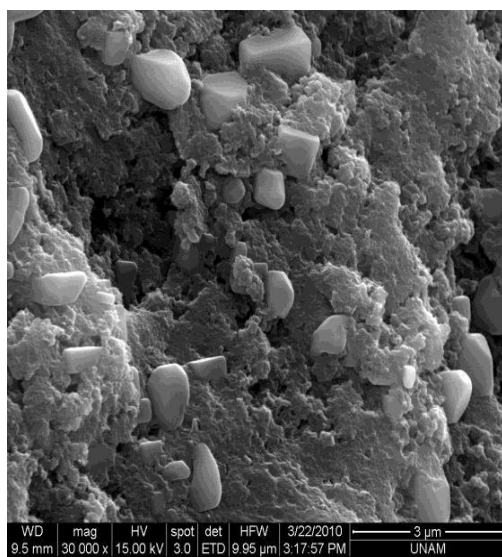
(b)
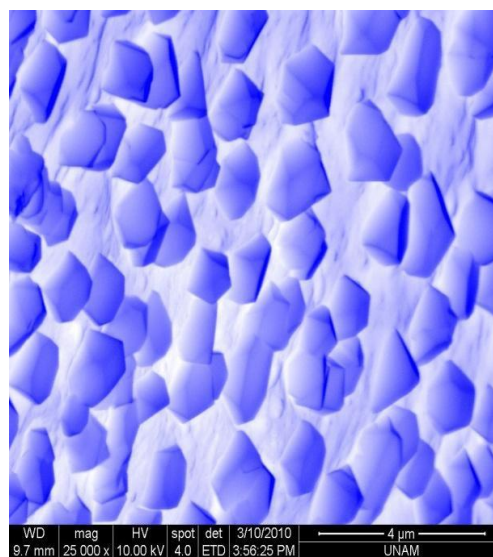
(c)

Figure 5. SEM images of (a) EC-*g*-AN-UO_2^{2+}, (b), and (c) EC-*g*-AO-UO_2^{2+} systems

Scheme 2. The orthorhombic bipyramidal crystal structure of UO_2^{2+}.

Using EDX as a non-destructive determination method, it is possible to perform a quantitative analysis of uranium in the organic or inorganic compounds. To this aim, EDX spectrum of UO_2^{2+} adsorbed EC-*g*-AO was taken simultaneously based on the SEM image. The surface was coated with gold (Au) for conductivity during the analysis. As indicated in Figure 6, the UO_2^{2+} attached sites are marked in red, and the copolymer surface is almost entirely covered by UO_2^{2+}. Starting from the low energy region, the bands observed for 0.4 keV and 0.5 keV were attributed to N K_α, and O K_α X-ray lines, respectively. Due to the copolymer surface coated with Au, bands observed at 2.120 keV, and 9.712 keV belong to Au M_α, and Au L_α X-ray lines, respectively. The EDX spectrum revealed two different lines depending on UO_2^{2+} adsorption: one is at 3.17 keV, which corresponds to U M_α, and the other is at 3.34 keV, belonging to U M_β. It is normal that the band intensities corresponding to the energy values are different because the UO_2^{2+} adsorption values obtained at different initial concentrations are different.
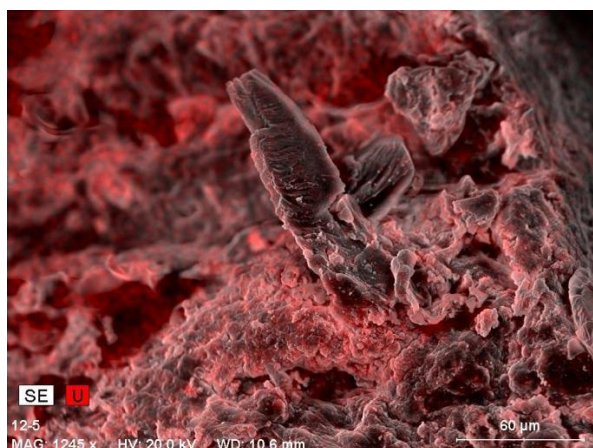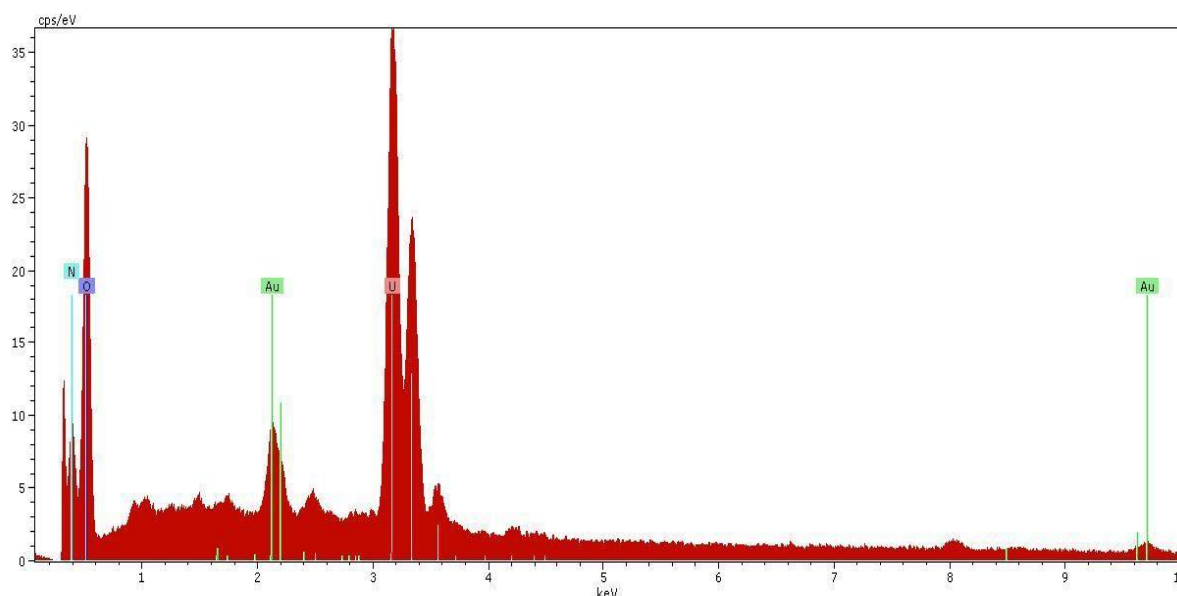
Figure 6. SEM-EDX spectrum of UO_2^{2+} adsorbed EC-*g*-AO copolymer (adsorption conditions: 800 mg/L UO_2^{2+}, 25°C, pH 4.1)

The final part of our study featured desorption experiments to determine the release of UO_2^{2+} from EC-*g*-AO copolymers. Certain amounts of UO_2^{2+} adsorbed EC-*g*-AO copolymers were separately added to 10 mL of EDTA, HCl, NaOH, and $NaHCO_3$ solutions (0.1 M each), and we measured, in regular intervals, the concentration of released UO_2^{2+} with UV-Vis spectrophotometer at 429 nm. The values of desorption (%) were calculated based on Equation 5. Table 3 indicates the total amounts of UO_2^{2+} (%) released from different desorption agent solutions. As can be seen in the table, $NaHCO_3$ is the most effective agent for desorption. Desorption of UO_2^{2+} from EC-*g*-AO copolymer in 0.1 M $NaHCO_3$ was found to be 52 %. A similar result was observed in the study conducted by Das *et al.* (13). In their study, amidoximated electron-beam-grafted polypropylene membranes were used for the uranium recovery; desorption of uranium from membrane was realized with 1.0 M $NaHCO_3$ with 85 % yield. Table 3 reveals another interesting point: We found that the desorption yield remained only at 52%. In our view, the low desorption yield might be due to the strong interaction between amidoxime groups close to the chemical adsorption boundary.

Table 3. Total release amounts (%) of UO_2^{2+} from EC-*g*-AO copolymers using different desorption agents.

mg UO_2^{2+} / g copolymer	Total UO_2^{2+} release (%)			
	0.1 M HCl	0.1. M EDTA	0.1 M NaHCO₃	0.1 M NaOH
240	17	12	52	13

CONCLUSIONS

The EC-*g*-AO copolymers are prepared by gamma irradiating binary mixtures of ethyl cellulose and acrylonitrile and subsequent amidoximation of the grafting chains. The adsorption behavior

of the uranyl ions in initial concentrations over a range of 100 – 1000 mg/L on the EC-*g*-AO copolymers is studied by the batch technique at a pH value of 4.1 at different temperatures. Interaction between UO_2^{2+} and amidoxime groups increases with increasing concentration of UO_2^{2+} at a given temperature. It can be found that the temperature induces a positive effect on the adsorption process and the adsorption capacity increases with an increase of UO_2^{2+} initial concentration. The findings suggested an adsorption capacity of 240 mg UO_2^{2+}/g dry copolymer. Desorption of adsorbed UO_2^{2+} ions from EC-*g*-AO copolymers was performed using different agents and it was found that $NaHCO_3$ is the most effective agent for desorption.

ACKNOWLEDGMENTS

REFERENCES

1. David Talbot: Uranium and lithium demand powers stocks. Available at http://www.theenergyreport.com/pub/na/10323.

2. Egawa H, Kabay N, Jyo A, Hirono M, Shuto T. Recovery of uranium from seawater.15. Development of amidoxime resins with high sedimentation velocity for passively driver fluidized bed adsorbers. Ind Eng Chem Res. 1994; 33:657-61.

3. Atia AA, Donia AM, Abou-El-Enein SA, Yousif AM. Studies on uptake   behaviour of copper(II) and lead(II) by amine chelating resins with different textural properties. 2003; Sep Purif Technol. 33:295-301.

4. Nilchi A, Babalou AA, Rafiee R, Sid Kalal H. Adsorption properties of amidoxime resins for separation of metal ions from aqueous systems. Reac Func Polym. 2008; 68:1665-70.

5. Liu X, Chen H, Wang C, Qu R et al. Adsorption properties of amidoximated porous acrylonitrile/methyl acrylate copolymer beads for Ag (I). Polym Adv Technol. 2011; 22:2032-8.

6. Tagami K, Uchida S. Use of TEVA resin for the determination of U isotopes in water samples by Q-ICP-MS. Appl Radiat Isotopes. 2004; 61:255-9.

7. Badawy SM, Sokker HH, Othman SH, Hashem A. Cloth filter for recovery of uranium from radioactive waste. Radiat Phys Chem. 2005; 73:125-130.

8. D'Souzaa SF, Sarb P, Kazyc SK, Kubala BS. Uranium sorption by Pseudomonas biomass immobilized in radiation polymerized polyacrylamide bio-beads. J Environ Sci Health, Part A. 2006; 41:487-500.

9. Chauhan GS, Kumar A. A study in the uranyl ions uptake on acrylic acid and acrylamide copolymeric hydrogels. J Appl Polym Sci. 2008; 110:3795-803.

10. O'Connell DW, Birkinshaw C, Dwyer TF. Heavy metal adsorbents prepared from the modification of cellulose: A review. Biores Technol. 2008; 99:6709-24.

11. Egawa H, Harada H. Recovery of uranium from seawater by using chelating resins containing amidoxime groups. Nippon Kagaku Kaishi. 1979; 958-9.

12. Rivas BL, Maturana HA, Villegas S. Adsorption behavior of metal ions by amidoxime chelating resin. J Appl Polym Sci. 2000; 77:1994-9.

13. Choi SH, Nho YC. Adsorption of UO_2^{+2} by polyethylene adsorbents with amidoxime, carboxyl, and amidoxime/carboxyl group. Radiat Phys Chem. 2000; 57:187-93.

14. Das S, Pandey AK, Athawale A, Kumar V, Bhardwaj YK, Sabharwal S, Manchanda VK. Chemical aspects of uranium recovery from seawater by amidoximated electron-beam-grafted polypropylene membranes. Desalination. 2008; 232:243-53.

15. Neti VS, Das S, Brown S, Janke CJ, Kuo L, Gill GA, Dai S, Mayes RT. Efficient functionalization of polyethylene fibers for the uranium extraction from seawater through atom transfer radical polymerization. Ind Eng Chem Res. 2017; 56:10826-32.

16. Abney CW. Mayes RT, Saito T, Dai S. Materials for the recovery of uranium from seawater. Chem Rev. 2017; 117:13935-14013.

17. Amphlett JTM, Ogden MD, Foster RI, Syna N, Soldenhoff K, Sharrad CA. Polyamine functionalisedion exchange resins: Synthesis, characterization and uranyl uptake. Chem Eng J. 2018; 334:1361-70.

18. Chau H, Yu P. Production of biodegradable plastics from chemical wastewater – A novel method to resolve excess activated sludge generates from industrial wastewater treatment. Water Sci Technol. 1999; 39:273-80.

19. Gupta KC and Sahoo S. Graft copolymerization of acrylonitrile and ethyl methacrylate comonomers on cellulose using ceric ions. Biomacromol. 2001; 2:239-47.

20. Gurgel LVA, Karnitz Jr O, de Freitas Gil RP, Gil LF. Adsorption of Cu(II), Cd(II), and Pb(II) from aqueous single metal solutions by cellulose and mercerized cellulose chemically modified with succinic anhydride. Biores Technol. 2008; 99:3077-83.

21. Akhtar K, Khalid AM, Akhtar MW, Ghauri MA. Removal and recovery of uranium from aqueous solutions by Ca-alginate immobilized Trichoderma harzianum. Biores Technol. 2009; 100:4551-8.

22. Zhou D, Zhang L, Zhou J, Guo S. Cellulose/chitin beads for adsorption of heavy metals in aqueous solution. Water Res. 2004; 38:2643-50.

23. Wang L, Dong W, Xu Y. Synthesis and characterization of hydroxy propylmethyl cellulose and ethyl acrylate graft copolymers. Carbohyd Polym. 2007; 68:626-36.

24. Başarır SŞ and Bayramgil NP. The uranium recovery from aqueous solutions using amidoxime modified cellulose derivatives. I. Preparation, characterization and amidoxime conversion of radiation grafted ethyl cellulose-acrylonitrile copolymers. Radiochim Acta. 2012; 100:893-9.

25. Qadeer R, Hanif J, Saleem M, Afzal M. Effect of alkali metals, alkaline earth metals and lanthanides on the adsorption of uranium on activated charcoal from aqueous solutions. J Radioanal Nucl Chem. 1992; 165:243-53.

26. Giles CH, MacEwan TH, Nakhwa SN, Smith D. Studies in adsorption. Part XI. A system of classification of solution adsorption isotherms, and its use in diagnosis of adsorption mechanisms and in measurements of specific surface areas of solids. J Chem Soc. 1960; 10:3973-93.

27. IUPAC Compendium Chem Terminology (1986) IUPAC. 58:448.

28. Bolster CH, Hornberger GM. On the use of linearized Langmuir equations. Soil Sci Soc Am J. 2007; 71:1796-1806, http://agris.fao.org/agris-search/search.do?recordID= US201300814267.

29. Saeed MM, Rusheed A, Ahmed N. Kinetics and thermodynamic aspect of the adsorption of Fe (III) on HTTA-imbedded polyurethane foam. J Radioanal Nucl Chem. 1996; 211:293-303.

30. Cou WH, Chao L, Zhu L. Efficient uranium(VI) biosorption on grapefruit peel: Kinetic study and thermodynamic parameters. J Radioanal Nucl Chem. 2012; 292:1303-15.

31. Li F, Tang Y, Wang HL, Yang JJ, Li SJ, Liu J, Tu H, Liao JL, Yang YY, Liu N. Functionalized hydrothermal carbon derived from waste pomelo peel as solid-phase extractant for the removal of uranyl from aqueous solution. Environmental Sci Poll Res. 2017; 24:22321-31.

32. Zohuriaan-Mehr MJ. Advances in chitin and chitosan modification through graft copolymerization: A comprehensive review. Iran Polym J. 2005; 14:235-65.

33. Nakajima A, Horikoshi T and Sakaguchi T. Recovery of uranium by immobilized microorganisms. Eur J Appl Microbiol Biotechnol. 1982; 16:88-91.

34. Gerente C, Andres Y and Le Cloirec P. Uranium removal onto chitosan: Competition with organic substances. Environ Technol. 1999; 20:515-21.

35. Na C, Park H, Kim B. Optimal amidoximation conditions of acrylonitrile grafted onto polypropylene by photoirradiation-induced graft polymerization. J Appl Polym Chem. 2012; 125:776-85.

36. Nyquist RA, Kagel RO. Infrared Spectra of Inorganic Compounds. Academic: New York, 1971; p 232.

37. Allen GC, Tempest PA. Ordered defects in the oxides of uranium. Proceedings of the Royal Society of London Series A. 1986; 406:325-44.